

Impact of spatially correlated noise on neuronal firing

Sentao Wang, Feng Liu,* and Wei Wang

National Laboratory of Solid State Microstructure and Department of Physics, Nanjing University, Nanjing 210093, China

Yuguo Yu

Center for the Neural Basis of Cognition, Carnegie Mellon University, Pittsburgh Pennsylvania 15213, USA

(Received 6 May 2003; revised manuscript received 30 September 2003; published 29 January 2004)

We explore the impact of spatially correlated noise on neuronal firing when uncoupled Hodgkin-Huxley model neurons are subjected to a common subthreshold signal. Noise can play a positive role in optimizing neuronal behavior. Although the output signal-to-noise ratio decreases with enhanced noise correlation, both the degree of synchronization among neurons and the spike timing precision are improved. This suggests that there can exist precisely synchronized firings in the presence of correlated noise and that the nervous system can exploit temporal patterns of neural activity to convey more information than just using rate codes. The mechanisms underlying these noise-induced effects are also discussed in detail.

DOI: 10.1103/PhysRevE.69.011909

PACS number(s): 87.16.Ac, 05.40.Ca

I. INTRODUCTION

Cortical spike trains with high interspike interval (ISI) variability have been observed in a wide range of stimulus-evoked activity of pyramidal neurons [1]. Moreover, the neural responses to repeated presentations of the same stimulus often vary largely from trial to trial [2]. An issue thus arises concerning how the nervous system can precisely process information. One often assumes that the response variability represents “neural noise” and that the averaged response over some populations of neurons may suppress the inherent noise and enhance the extracted information about the stimulus. But such a hypothesis is based on the condition that the response variation in each neuron is more or less independent of that in its neighbors [2,3]. However, it has been demonstrated that neural populations can exhibit significant covariance both in their spontaneous and stimulus-evoked activity [4,5].

It has been suggested that, in the presence of correlation in response variation, one possible function for neurons to carry redundant message may be to improve the temporal resolution in coding a rapidly changing variable [6]. That is, temporal correlations are crucial for signal processing as part of the information is encoded in the temporal structure of activity patterns. Furthermore, the synchronized activities of neurons with high temporal precision can be transmitted more efficiently than the asynchronous ones [7]. It has also been argued [8] that cortical neurons might act more as coincidence detectors preferentially relaying synchronized activity, than as temporal integrators effectively summing incoming synaptic inputs. However, how the synchronization and coincidence-detection mechanisms work in as noisy an environment as a cortical circuit remains elusive.

It is well known that cortical neurons are subjected to large numbers of random synaptic inputs and other endogenous noise. As a first approximation, we can model these together as Gaussian noise. But as mentioned above, cortical neurons display coherence in their firing activity, and thus

the correlation in input noise must be taken into account. It has recently been shown that noise can play a constructive role in weak signal detection, such as improving the output signal-to-noise ratio (SNR), in the context of stochastic resonance (SR) [9]. While we have previously discussed the impact of spatially correlated noise on the output SNR [10], here we mainly explore its influence on neuronal synchronization and spike timing precision, as well as their biological relevance.

Motivated by the aforementioned considerations, we construct a network composed of uncoupled neurons which are subjected to a common subthreshold (local field potential) signal $s(t)$ plus spatially correlated noise $\eta(t)$. The neural behavior depends remarkably on both noise intensity D and the measure R of noise correlation. On the one hand, the output SNR, the population coherence measure, and the spike timing precision all go through a maximum as a function of D . On the other hand, the SNR monotonically decreases with increasing R , whereas both the degree of synchronization among the neurons and the spike timing precision are improved. This makes it possible for neural networks to exploit precise spatiotemporal firing patterns to encode the stimulus. The mechanisms underlying these noise-induced effects are also discussed in detail. This paper is organized as follows. The model is described in Sec. II, while the results and discussion are presented in Sec. III. Finally, a conclusion is given in Sec. IV.

II. MODEL

We consider a summing network composed of Hodgkin-Huxley (HH) model neurons which are connected in parallel and converge to a summing center Σ , as shown in Fig. 1. The dynamic equations for the network are presented as follows [11]:

$$C_m \frac{dV_i}{dt} = -g_{N_a} m_i^3 h_i (V_i - E_{N_a}) - g_{K} n_i^4 (V_i - E_K) - g_l (V_i - E_l) + I_0 + s(t) + \eta_i(t), \quad (1)$$

$$\frac{dm_i}{dt} = \alpha_m(V_i)(1 - m_i) - \beta_m(V_i)m_i, \quad (2)$$

*Corresponding author. Email address: fliu@nju.edu.cn

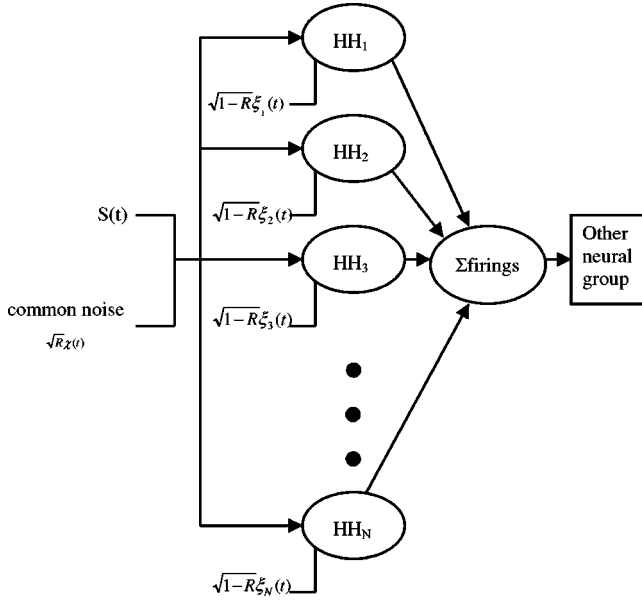


FIG. 1. A schematic diagram of the network composed of HH neurons. The total noise is divided into two items: the common noise $\sqrt{R}\chi(t)$ and the independent noise $\sqrt{1-R}\varepsilon_i(t)$.

$$\frac{dh_i}{dt} = \alpha_h(V_i)(1-h_i) - \beta_h(V_i)h_i, \quad (3)$$

$$\frac{dn_i}{dt} = \alpha_n(V_i)(1-n_i) - \beta_n(V_i)n_i, \quad i=1, \dots, N. \quad (4)$$

Here $C_m = 1 \mu\text{F}/\text{cm}^2$, $E_{N_a} = 50 \text{ mV}$, $E_K = -77 \text{ mV}$, $E_l = -54.4 \text{ mV}$, $g_{N_a} = 120 \text{ mS}/\text{cm}^2$, $g_K = 36 \text{ mS}/\text{cm}^2$, $g_l = 0.3 \text{ mS}/\text{cm}^2$, and $\alpha_m(V) = 0.1(V+40)/(1-e^{-(V+40)/10})$, $\beta_m(V) = 4e^{-(V+65)/18}$, $\alpha_h(V) = 0.07e^{-(V+65)/20}$, $\beta_h(V) = 1/(1+e^{-(V+35)/10})$, $\alpha_n(V) = 0.01(V+55)/(1-e^{-(V+55)/10})$, and $\beta_n(V) = 0.125e^{-(V+65)/80}$. All the currents are in units of $\mu\text{A}/\text{cm}^2$.

I_0 is a constant bias and taken as $1 \mu\text{A}/\text{cm}^2$. $s(t)$ is a subthreshold signal, $A \cos(2\pi f_s t)$, corresponding to the input generated by the local field potential. The signal frequency is set to $f_s = 50 \text{ Hz}$ unless specified otherwise, and the signal amplitude is $A = 1 \mu\text{A}/\text{cm}^2$. Similar to that in Refs. [10,12], the noise term is assumed to be $\eta_i(t) = \sqrt{1-R}\varepsilon_i(t) + \sqrt{R}\chi(t)$ with

$$\langle \varepsilon_i(t) \rangle = 0, \quad \langle \varepsilon_i(t_1) \varepsilon_j(t_2) \rangle = 2D \delta_{ij} \delta(t_1 - t_2), \quad (5)$$

and

$$\langle \chi(t) \rangle = 0, \quad \langle \chi(t_1) \chi(t_2) \rangle = D \lambda e^{-\lambda|t_1 - t_2|}. \quad (6)$$

Here $\langle \rangle$ represents the ensemble average and D is referred to as noise intensity. $\varepsilon_i(t)$ is the independent Gaussian white noise, while $\chi(t)$ is the Gaussian colored noise with the correlation time λ^{-1} being 2 ms. Since

$$\langle \eta_i(t_1) \eta_j(t_2) \rangle = 2D(1-R) \delta_{ij} \delta(t_1 - t_2) + RD \lambda e^{-\lambda|t_1 - t_2|}, \quad (7)$$

the control parameter R ($0 \leq R \leq 1$) measures the noise correlation between a pair of neurons. In the above assumption, we can consider that $\varepsilon_i(t)$ represents the internal noise, while $\chi(t)$ reflects the random synaptic input from neurons beyond the system under study. This is plausible when we model cortical neurons in the same column. It has been stressed in Ref. [5] that common input, common stimulus selectivity, and common noise are tightly linked in functioning cortical circuits.

The output of the network is defined as

$$I^{out}(t) = \frac{1}{N} \sum_{i=1}^N \theta(V_i(t) - V^*). \quad (8)$$

V^* is the firing threshold taken as -20 mV , and $\theta(x) = 1$ if $x \geq 0$ and $\theta(x) = 0$ if $x < 0$. Thus the summer (Σ) operates by averaging the output spike train of each unit to obtain a resultant output for the entire system. The number of neurons in the network is set to $N = 500$ unless specified otherwise. The output SNR is defined as $10 \log_{10}(S/B)$ with S and B representing the signal peak and the mean amplitude of the noise at the input signal frequency in the power spectrum for $I^{out}(t)$, respectively. Numerical integration is performed by a second-order stochastic algorithm [13], and the time step is $500/32768 \text{ ms}$. An average over 50 different realizations is taken to obtain reported results.

III. RESULTS AND DISCUSSION

First, we investigate the influence of spatially correlated noise on neuronal firing. For $R = 1$, since all the neurons are subjected to an identical input, they discharge at the same time but the firings exhibit skipping as seen in Fig. 2(a). That is, $I^{out}(t)$ is composed of irregular sequences of ones and zeros. In contrast, for the case of independent noise ($R = 0$), while one neuron is responding poorly to the signal without spiking, others may be responding well. As a result, $I^{out}(t)$ varies nearly periodically at the same frequency as the signal though its peak values are small. For $0 < R < 1$, however, $I^{out}(t)$ exhibits apparent fluctuations between different driving cycles; that is, $I^{out}(t)$ is nearly zero in some driving cycles, whereas it takes a relatively high value in others. Such fluctuations become more remarkable with increasing R . This means that more neurons tend to fire simultaneously as the correlation in input noise is enhanced. In other words, the neurons exhibit synchronous firing but meanwhile the ISIs are more variable. It is noted that $\sqrt{R}\chi(t)$ has a dominant impact on neuronal firing compared to $\sqrt{1-R}\varepsilon_i(t)$ when $R > 0.5$.

Figure 2(b) depicts the output SNR against noise intensity D for different values of R . Each curve presents a typical characteristic of the SR, namely, the SNR goes through a maximum with increasing D . The optimal noise intensity slightly shifts rightward as R increases. Note that at each noise level the SNR is rigorously a decreasing function of R . This is clearly shown in Fig. 2(c). In fact, in the case of independent input noise, population averaging can effectively suppress the inherent noise, and thus the output signal contains more information about the stimulus. In contrast, in

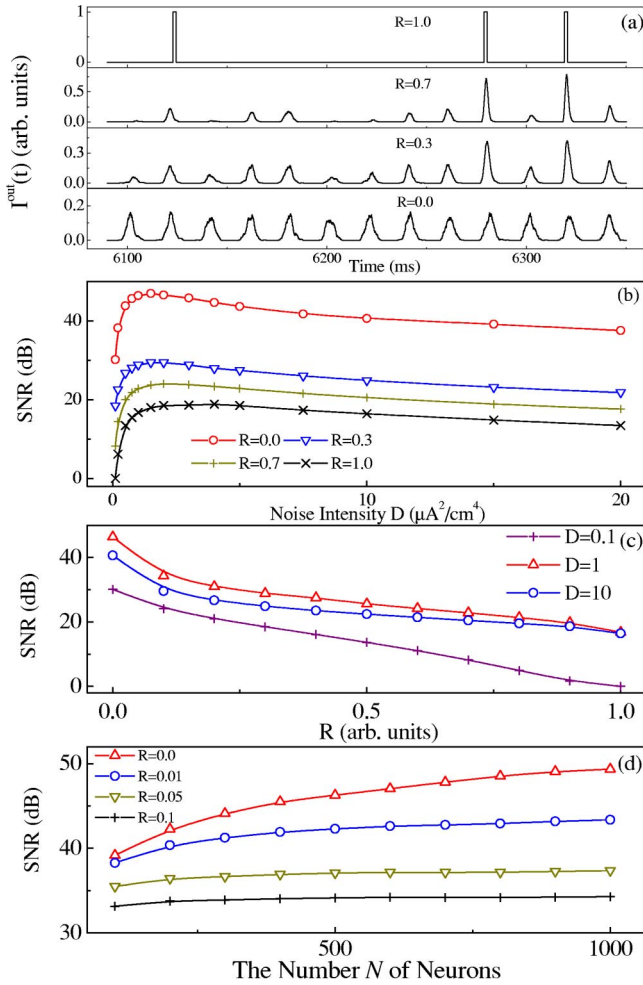


FIG. 2. (a) $I^{out}(t)$ vs time (with $D=1$) and (b) the output SNR vs noise intensity for $R=0.0, 0.3, 0.7,$ and $1.0,$ respectively. (c) The output SNR vs the measure R of noise correlation for $D=0.1, 1,$ and $10,$ respectively. (d) The output SNR vs the network size for $R=0.0, 0.01, 0.05,$ and $0.1,$ respectively, with $D=1.$

the case of spatially correlated noise, the averaged activity is nearly as noisy and variable as that of individual neurons. Thus the SNR decreases evidently compared to that for $R=0.$ These imply that, in terms of the SNR, improving the correlation in input noise instead diminishes the beneficial effect of population averaging as reported in Ref. [10]. It has also been demonstrated that positive noise correlation decreases the estimation capacity of the network in the light of a Fisher information measure [14].

Moreover, pooling more neurons has a minor influence on improving the SNR in the presence of noise correlation [see Fig. 2(d)]. For $R=0,$ the SNR first increases apparently with the ensemble size N and is saturated at large $N (> 1000).$ But provided there is little correlation in the noise, the SNR rises slightly or nearly remains constant with increasing $N.$ Thus it seems unlikely to enhance the performance of the averaged activity by pooling more neurons in the light of the SNR. Nevertheless, this also indicates that the neurons exhibit strong synchronization when subjected to correlated noise input.

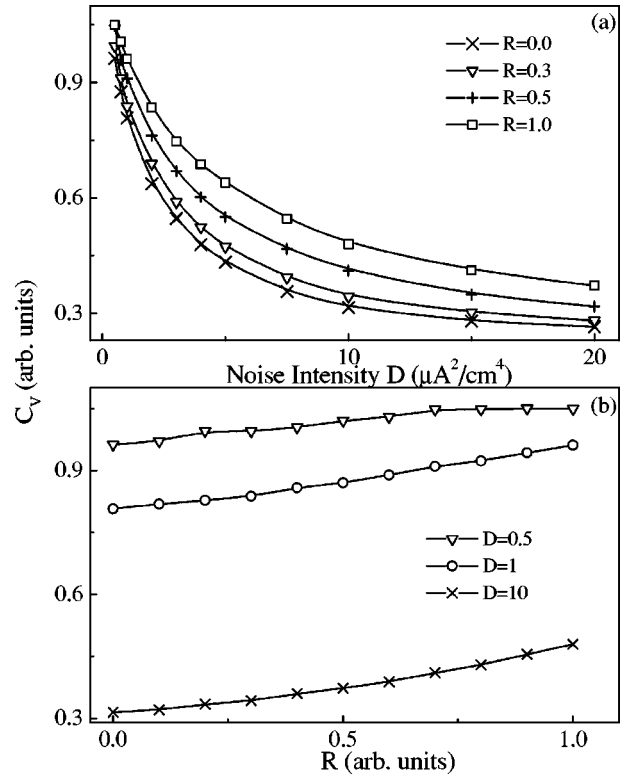


FIG. 3. (a) C_v vs noise intensity D for $R=0.0, 0.3, 0.5,$ and $1.0,$ respectively. (b) C_v vs R for $D=0.5, 1,$ and $10,$ respectively.

The most common way to characterize the ISI variability is via the coefficient of variation (C_v) of interspike intervals, which is defined as the ratio of the standard deviation to the mean of ISI. Figure 3(a) depicts C_v against noise intensity for different values of $R.$ For each R, C_v is a monotonically decreasing function of D (for $D \geq 0.5).$ This is in agreement with the results shown in Ref. [15] (cf. Fig. 4 therein). It is noted that C_v is an increasing function of R as seen in Fig. 3(b). This means that the spike sequences become more variable with increasing the correlation in input noise.

It is noted that the above conclusions also hold for various signal frequencies. Figure 4(a) depicts the SNR against R for different values of $f_s.$ The SNR always declines monotonically with $R.$ But the neurons display different firing coherence with the signal. As a result, the SNR takes a relatively large value for $30 \leq f_s \leq 100$ Hz [see Fig. 4(b)]. That is, the neurons are more sensitive to the signals with frequencies ranging from 30 to 100 Hz. Such frequency sensitivity has also been reported in Ref. [16] and results from the resonance effect between the subthreshold oscillation of membrane potential and the periodic signal. Resonance improves the ability of neurons to respond selectively to inputs at preferred frequencies. As a matter of fact, the resonance and frequency preference may be one of the basic principles underlying cognitive and behavioral processes.

To quantify the synchronization between neurons, we use a coherence measure based on the normalized cross correlations of their spike trains at zero time lag [17]. To be specific, supposing that a long time interval T is divided into small bins of τ and that two spike trains are given by $X_i(t) = 0$ or

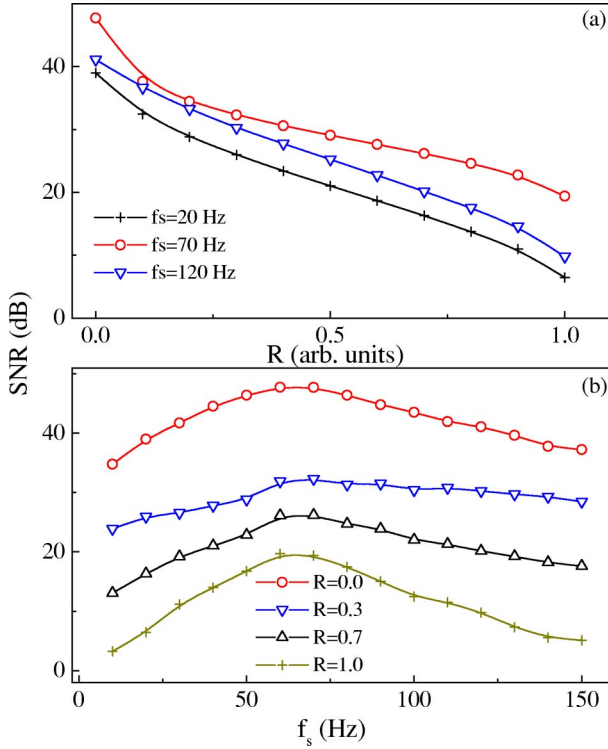


FIG. 4. $D=1$. (a) The output SNR vs R for the signals with $f_s=20$, 70, and 120 Hz, respectively. (b) The output SNR vs the signal frequency for $R=0.0$, 0.3, 0.7, and 1.0, respectively.

1 and $X_j(l)=0$ or 1, with $l=1,2,\dots,m$ (here $T/m=\tau$). The coherence measure for the pair is then defined as

$$K_{ij}(\tau) = \frac{\sum_{l=1}^m X_i(l)X_j(l)}{\sqrt{\sum_{l=1}^m X_i(l) \sum_{l=1}^m X_j(l)}}. \quad (9)$$

The population coherence measure K is obtained by averaging K_{ij} over all pairs of the neurons in the network. Here τ is taken as 2 ms.

Figure 5(a) plots K versus noise intensity D . K goes through a maximum as a function of D , namely, there also exists an optimal noise level for the neuronal synchronization. Furthermore, this optimal noise intensity is nearly identical to that for the SNR shown in Fig. 2(b). Note that K is higher in the case of $R=0.7$. In fact, K is an increasing function of R as seen in Fig. 5(b). Therefore, the level of synchronization among the neurons is indeed improved by increasing the noise correlation.

We have discussed the neural firing under different conditions of input noise and found that the spatially correlated noise enhances the degree of synchronized firing. Now we examine in detail the impact of noise correlation on spike timing. Figure 5(c) plots poststimulus time histograms (PSTHs), which characterize the number of spikes collected at the summer per millisecond [11]. It is in essence equivalent to $I^{out}(t)$ showing how the neurons fire synchronously over time. Obviously, there are many peaks located around

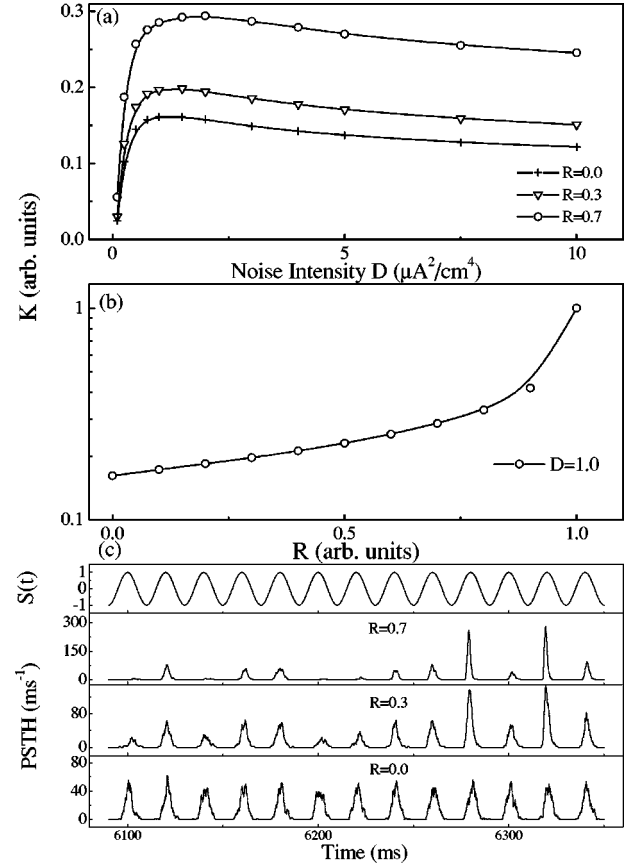


FIG. 5. (a) The population coherence K vs noise intensity for $R=0.0$, 0.3, and 0.7, respectively. (b) K vs R with $D=1$. (c) The input signal $s(t)$ and PSTHs for $R=0.0$, 0.3, and 0.7, respectively, with $D=1$.

the maxima of the signal, indicating a phase locking to the stimulus. In the case of independent noise, the peaks in each cycle are nearly of the same short height, meaning that the neurons show weak synchronization. When the noise correlation is enhanced, the degree of synchronization among the neurons is evidently improved as the PSTH takes a large value in some driving cycles but a much smaller one in others. As R further increases, those high peaks prominently rise while the fluctuations become more remarkable. These results are in agreement with those shown in Fig. 2(a).

As mentioned above, in temporal coding the precise timing of spikes is used to encode a stimulus. Thus the reliability and precision of firing patterns is a dominant factor determining the quality of a temporal code. Based on the shape of a smoothed data set taken from a five-point moving average of the PSTH, the spike timing precision is defined as [18]

$$P_i = H_i / w_i, \quad (10)$$

where H_i is the height of the i th peak in the smoothed PSTH, and w_i is the width at H_i/e . The mean precision P is obtained by an average over 200 driving cycles. Clearly, P quantitatively characterizes the average number of spikes and their coincidence in any firing event in the PSTH.

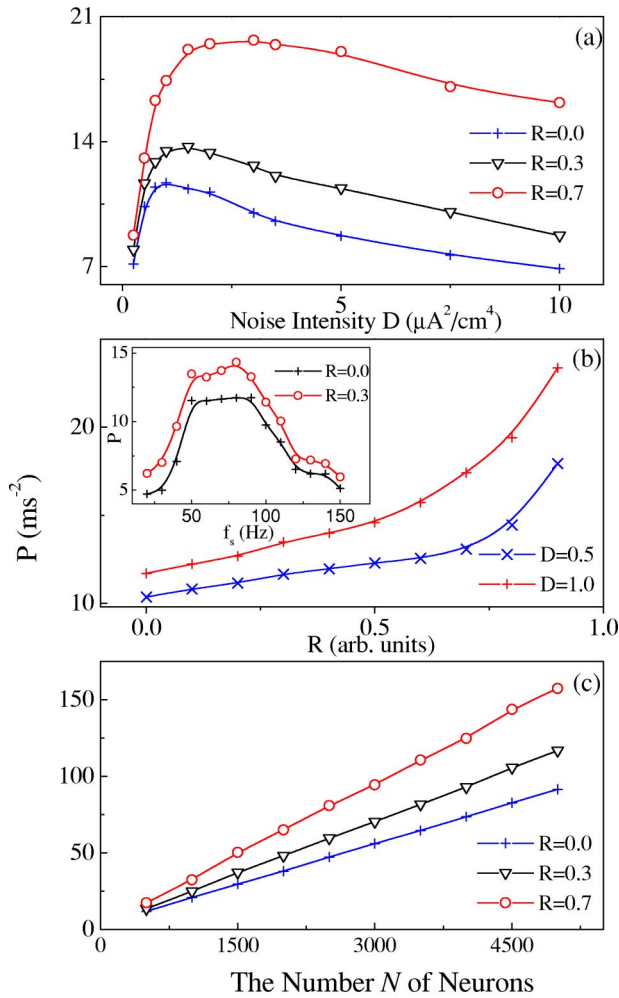


FIG. 6. (a) The spike timing precision P vs noise intensity for $R=0.0, 0.3$, and 0.7 , respectively. (b) P vs R for $D=0.5$ and 1.0 , respectively. The inset is P vs the signal frequency f_s for $R=0.0$ and 0.3 , respectively, with $D=1$. (c) P vs the network size for $R=0.0, 0.3$, and 0.7 , respectively, with $D=1$.

Figure 6(a) shows P versus noise intensity D for various values of R . Each curve displays a SR-like behavior. That is, there exists an optimal noise level which maximizes the timing precision via the SR mechanism. This indicates that the spike timing precision in response to subthreshold periodic stimuli can be enhanced by input noise, as reported in Ref. [18]. The optimal noise intensity also slightly shifts rightward with increasing R . Moreover, for each R the maximum SNR, K , and P occur at the same noise intensity. These verify that noise can play a positive role in weak signal processing. The timing precision also monotonically increases with R [see Fig. 6(b)], which means that the correlated noise does make the spike timing more precise. It is noted that P increases more steeply when $R > 0.5$ since $\sqrt{R}\chi(t)$, the dominant part of the noise, makes the neurons prone to fire synchronously. The inset of Fig. 6(b) depicts P against the signal frequency for $D=1$. Clearly, P takes a relatively large value for $50 \leq f_s \leq 90$ Hz. This indicates that the neurons transmit these signals with a high precision and respond preferentially to them.

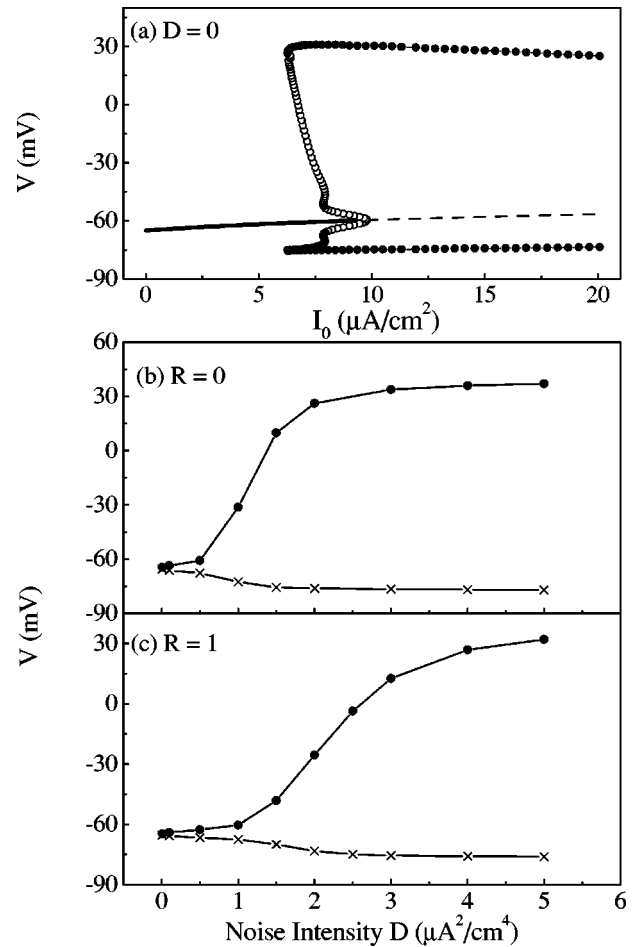


FIG. 7. (a) Deterministic bifurcation diagram of a HH neuron under dc current input. Here I_0 is the bifurcation parameter and V is the membrane potential. The thick and dashed lines represent stable and unstable fixed points, respectively. The filled and open circles represent both maxima and minima of stable and unstable limit cycles, respectively. Noise-induced bifurcation diagram for $R=0$ (b) and $R=1$ (c). The curves represent the upper (●) and lower (×) bounds of the stationary distribution of membrane potential for each noise intensity D .

It is worth noting that the timing precision linearly increases with the number of neurons and that the slope rises with increasing R , which is clearly seen in Fig. 6(c). This is largely different from the dependence of the output SNR on N shown in Fig. 2(d). Here we see that pooling more neurons is of functional significance in effectively firing postsynaptic neurons, and this effect is more prominent in the case of correlated noise.

It is of interest to investigate the mechanism underlying these noise-induced effects. We first discuss the bifurcation in the HH neuron to a constant bias I_0 in the absence of noise ($D=0$) and input signal ($A=0$). As seen in Fig. 7(a), for $I_0 < I_c = 6.2$ there is only a globally stable fixed point. The birth of stable and unstable limit cycles occurs at I_c due to the saddle-node bifurcation. For $I_c < I_0 < I_h = 9.8$, there exist a stable fixed point, a stable limit cycle, and an unstable limit cycle. The unstable limit cycle constitutes the boundary separating the attractive basins corresponding to the fixed

point and limit cycle. When the initial condition V_0 falls inside this boundary, i.e., in the contraction region, the dynamics of system will be attracted to the point attractor. If V_0 is outside the boundary, i.e., in the expansion region, the system will be attracted to the stable limit cycle. As we shall see, this feature has a large impact on neuronal synchronization. At $I_0=I_h$ the Hopf bifurcation occurs and there is only a stable limit cycle thereafter.

In the presence of noise, the neurons can be evoked to discharge spikes, and there exists a noise-induced transition in excitability with increasing D [19]. To quantify such a transition, we compute stochastic bifurcation diagram in the same way as in Refs. [19,20]. Figures 7(b) and 7(c) show the noise-evoked transition diagrams for $R=0$ and $R=1$, respectively, providing a global view of how the stationary distribution V_{99} of membrane potential changes with D . For each fixed D , output membrane potential has been collected for 100 s. Then the top and bottom limits of the distribution are computed in the way so that 99% of the distribution is below the upper line and 99% is above the lower one. Three regions can be distinguished. For $R=0$, the distribution increases linearly for low noise ($D \leq 0.5$). As noise intensity increases ($0.5 < D \leq 2$), the distribution evidently widens. That is, a transition occurs around $D=0.5$. When D is further increased, the distribution changes slightly. For $R=1$, however, the bifurcation point is shifted rightwards and the second region also broadens. Tanabe *et al.* [19] demonstrated that noise with intensities prior to the bifurcation point may play an important role in enhancing spike timing precision. Here we further show that the correlation of noise widens this beneficial region, which can largely enhance the neuronal synchronization and lead to high variability of the spiking dynamics.

Comparing Figs. 2(b), 5(a) and 6(a) with Figs. 7(b) and 7(c), we see that the SNR, K , and P are in step with the distribution of membrane potential varying with D . Thus we can interpret their dependence on D and R in terms of the excitability of neurons. In the first regime, noise-induced fluctuations improve the excitability of some units in the ensemble, while their membrane potentials are located around the resting potential. In the presence of input signal, those neurons which are more excitable than at rest may fire synchronously in some driving cycles. As noise is increased within this range, more neurons evolve closer to the firing threshold, and enhanced response is observed such as the rise of the SNR and P . As the noise is further increased beyond the first regime, the membrane potential fluctuations evidently increase. A fraction of neurons that are evoked to fire by noise alone may not respond to the input due to the refractory period, while other neurons whose membrane potentials are around the resting potential may be triggered to fire simultaneously by the signal. This may reduce the overall response of the ensemble. In the third regime with larger noise intensity, the noise fluctuations become dominant, and the neural coherence further decreases. Here the boundary between attractive basins, which is related to the unstable limit cycle, plays a crucial role in the noise-induced synchronization, as reported in Ref. [21] wherein a saddle point embedded in system dynamics is responsible for the noise-

evoked synchronization. It is worth noting that in the case of correlated noise, the first region evidently expands, and this gives rise to a prominent increment in P and K with increasing D .

Therefore, the correlated noise has two primary effects on neuronal firing. The first is related to noise intensity. In the absence of input signal, small noise disturbs the long-term motion of the system and results in the dominance of contraction dynamics. The membrane potential is distributed in a narrow region. In this case, the noise can trigger the neurons to respond synchronously to a weak signal, leading to a higher spike timing precision when noise intensity is increased up to the transition point. For large noise intensity, the membrane potential distribution is largely broadened. In this case, when the weak signal is input to the system, noise-induced firings become dominant while the effect of the signal on driving the ensemble in phase has been disturbed heavily. This leads to a decrease of spike timing precision with increasing D .

The second effect of noise is due to its correlation. For a fixed noise intensity, neurons with independent noise can fire spikes more independently, whereas correlation in noise makes the neurons prone to act together, which increases the inertia of ensemble neurons to be rest or to fire synchronously. That is, the correlation drives neurons with different initial conditions to converge to an identical response, being inside the contraction or expansion region. This results in an enhanced neural synchronization. Periodic signal plays a similar synergic role to correlation in driving the neural dynamics in phase, improving the level of synchronization among neurons.

Finally, it is worth noting that the correlation of noise not only enhances spike timing precision [see Fig. 6(a)], but also enlarges the spiking variability [see Fig. 3(b)]. The increment in ISI variability will improve the encoding capacity of neurons. This is of functional significance when considering how the nervous system tunes noise intensity to its optimal values. Our results may give a reasonable mechanism for why neural responses in the cerebral cortex often become highly variable but precise in encoding input signals [1].

IV. CONCLUSION

We have demonstrated that there exists precisely synchronized activity in the presence of strong noise correlation. Our results reproduce some of the typical firing characteristics observed in cortical neurons. First, it is generally agreed that the response variability originates in unreliable synaptic inputs [22]. We also showed that the spike sequences become more variable in response to correlated noise. Second, large-scale synchronized firings have been observed in a variety of brain areas, especially the γ oscillations (at frequencies of 30–70 Hz) [23], which play functional roles such as pattern segmentation and feature binding. The frequency sensitivity shown in Figs. 4 and 6(b) may give us an enlightenment why the γ oscillations are so ubiquitous in the nervous system. Third, it has been found that under some conditions the spike timing can show a high precision and reproducibility with the temporal resolution being 2–3 ms [24]. Thus precise

temporal firing patterns can be exploited to encode the stimulus.

As shown in Fig. 2(a), although the neurons exhibit synchronized firings when $R=0.7$, they miss firing in many driving cycles. But this does not necessarily mean that the neurons are poorly processing information. In contrast, such synchronized activity may subserve information processing. For example, $s(t)$ may just represent a modulation of neural behavior providing the system with an effect of frequency selection [16], and the neurons may preferentially respond to synchronized synaptic inputs. Alternatively, the neural networks can exploit precise temporal relations among neurons to select responses for joint processing and to bind neurons temporally into functionally coherent assemblies [7]. Furthermore, the combination of synchronized firing of cortical neurons and high temporal precision also makes it possible for their downstream neurons to act as coincidence detectors preferentially transferring synchronized activity [8]. For instance, a coincidence-detection neuron can precisely determine whether two coupled neurons receive similar level of sensory input [25].

Although we did not directly model the random synaptic input, our results suggest that the noise correlation is crucial for cortical neurons to temporally process information and that the cerebral cortex may convey more information via temporal codes than exclusively using rate codes. In contrast, it seems plausible to assume that sensory neurons in the peripheral nervous system are subject to more or less independent noise. In that case, it is the averaging of neural responses that encodes a stimulus feature such as the signal frequency.

In addition, it is noted that Rudolph and Destexhe inves-

tigated the case wherein a neuron is subjected to a periodic weak signal plus large numbers of random synaptic inputs [26]. They reported that neuronal response can also be enhanced by the correlation among synaptic inputs, exhibiting a SR-like behavior. Their results suggested that cortical neurons are efficient in detecting such correlations within millisecond time scales. This is consistent with the present work that neurons may exploit correlated noise to encode and transmit information.

In conclusion, in this paper we have explored the impact of spatially correlated noise on neuronal firing. Noise can play a constructive role in optimizing neuronal response to subthreshold stimuli. The results illustrate how the presence of correlated noise improves the degree of synchronization among the neurons and the spike timing precision but meanwhile makes output spikes more variable. With a high timing resolution, temporal structures of neural activity can be used to convey more information. Thus correlated firings of neurons play functional roles in signal processing. These results are consistent with observations in cortical neurons and imply that we should consider the correlation in noise or synaptic input when we model the cortical dynamics. Finally, we would like to point out that the present form of noise is a simplification, and it is of interest to exploit more complex configurations, such as the spatially decaying functions over the population.

ACKNOWLEDGMENTS

This work was supported by the National Natural Sciences Foundation of China (under Grant No. 30070208) and the Nonlinear Science Project of NSM.

-
- [1] W. Softky and K. Koch, *J. Neurosci.* **13**, 334 (1993); M.N. Shadlen and W.T. Newsome, *ibid.* **18**, 3870 (1998).
 - [2] D. Ferster, *Science* **273**, 1812 (1996).
 - [3] E. Zohary, M.N. Shadlen, and W.T. Newsome, *Nature (London)* **370**, 140 (1994); M.N. Shadlen, K.H. Britten, W.T. Newsome, and J.A. Movshon, *J. Neurosci.* **16**, 1486 (1996).
 - [4] A. Arieli, D. Shoham, R. Hildesheim, and A. Grinvald, *J. Neurophysiol.* **73**, 2072 (1995); A. Arieli, A. Sterkin, A. Grinvald, and A. Aertsen, *Science* **273**, 1868 (1996).
 - [5] W. Bair, E. Zohary, and W.T. Newsome, *J. Neurosci.* **21**, 1676 (2001).
 - [6] D. Lee, N.L. Port, W. Kruse, and A.P. Georgopoulos, *J. Neurosci.* **18**, 1161 (1998).
 - [7] W. Singer, *Curr. Opin. Neurobiol.* **9**, 189 (1999).
 - [8] P. König, A.K. Engel, and W. Singer, *Trends Neurosci.* **19**, 130 (1996).
 - [9] L. Gamaitoni, P. Hänggi, P. Jung, and F. Marchesoni, *Rev. Mod. Phys.* **70**, 223 (1998).
 - [10] F. Liu, B. Hu, and W. Wang, *Phys. Rev. E* **63**, 031907 (2001).
 - [11] Y. Yu, F. Liu, J. Wang, and W. Wang, *Phys. Lett. A* **282**, 23 (2001).
 - [12] C. Zhou, J. Kurths, and B. Hu, *Phys. Rev. Lett.* **87**, 098101 (2001).
 - [13] R.F. Fox, *Phys. Rev. A* **43**, 2649 (1991).
 - [14] H. Sompolinsky, H. Yoon, K. Kang, and M. Shamir, *Phys. Rev. E* **64**, 051904 (2001).
 - [15] J. Feng and P. Zhang, *Phys. Rev. E* **63**, 051902 (2001).
 - [16] Y. Yu, W. Wang, J. Wang, and F. Liu, *Phys. Rev. E* **63**, 021907 (2001); F. Liu, J.F. Wang, and W. Wang, *ibid.* **59**, 3453 (1999).
 - [17] X. Wang and G. Buzsaki, *J. Neurosci.* **16**, 6402 (1996).
 - [18] X. Pei, L. Wilkens, and F. Moss, *Phys. Rev. Lett.* **77**, 4679 (1996).
 - [19] S. Tanabe, S. Sato, and K. Pakdaman, *Phys. Rev. E* **60**, 7235 (1999).
 - [20] S. Tanabe and K. Pakdaman, *Biol. Cybern.* **85**, 269 (2000).
 - [21] C. Zhou and J. Kurths, *Chaos* **13**, 401 (2003).
 - [22] J.A. Movshon, *Neuron* **27**, 412 (2000).
 - [23] *Neuron* **24**, 7 (1999), special issue on the binding problem, edited by A. Roskies.
 - [24] W. Bair and K. Koch, *Neural Comput.* **15**, 1185 (1996); A. Riehle, S. Grün, M. Diesmann, and A. Aertsen, *Science* **278**, 1950 (1997).
 - [25] L.F. Abbott, *Nat. Neurosci.* **4**, 115 (2001); J.J. Hopfield and C.D. Brody, *Proc. Natl. Acad. Sci. U.S.A.* **97**, 13 919 (2000).
 - [26] M. Rudolph and A. Destexhe, *Phys. Rev. Lett.* **86**, 3662 (2001); *J. Comput. Neurosci.* **11**, 19 (2001).